Cross sections for electron-impact excitation of krypton from the levels of $4p^6$, $4p^55s$, and $4p^55p$ configurations

Jiaolong Zeng,[1,2] Jianhua Wu,[2] Fengtao Jin,[2] Gang Zhao,[1] and Jianmin Yuan[1,2]
[1]*National Astronomical Observatories, Chinese Academy of Sciences, Datun Road 20A, Chaoyang, Beijing 100012, People's Republic of China*
[2]*Department of Applied Physics, National University of Defense Technology, Changsha 410073, People's Republic of China*
(Received 13 June 2005; published 14 October 2005)

The electron-impact excitation cross sections at low electron energies have been calculated using a fully relativistic *R*-matrix method for transitions between levels of $4p^6$, $4p^55s$, and $4p^55p$ configurations. To ensure the convergence of results, we have paid special attention to the factors that may affect the convergence of cross sections. For examples, we have included extensive configuration interactions in the wave-function expansion of the target states. A large enough *R*-matrix boundary has been taken to ensure the convergence of atomic wave functions. Contributions to cross sections from a large number of partial waves (up to $J=39.5$) have been explicitly calculated. The final results are in good agreement with recent experimental data by Jung *et al.* [Phys. Rev. Lett. **94**, 163202 (2005)] after shifting the position of electron energy. The relative difference is about 10% for four transitions out of the metastable levels. The results eliminated the significant discrepancies between theory and experimental work on excitation cross sections out of the metastable levels reported in the literature.

DOI: 10.1103/PhysRevA.72.042707 PACS number(s): 34.80.Dp

I. INTRODUCTION

Electron collision processes with the rare gases have been a topic of continuous interest for both fundamental and practical reasons. They help us to understand basic electron-atom interactions and have applications to many fields such as gas lasers, plasma processing, and lighting technology, etc. In addition, electron-impact excitation cross sections are also very important in calculating the width and shift of spectral lines in a method of quantum mechanics. Recently, Milosavljevic and Djenize [1] experimentally measured the electron-impact widths of neutral krypton in transitions of $5s$-$5p$ and $5s$-$6p$. They theoretically calculated the widths by using a semiclassical method. More accurate treatment of the widths and shifts caused by electron impact should use a method of quantum mechanics.

The recent interest in this field has attracted a lot of researchers to study the electron-impact excitation cross sections of Kr, both theoretically and experimentally. Experimentally, Fel'tsan [2] measured the optical emission cross sections for transitions of the type $4p^55p$-$4p^55s$. Cross sections for only a few transitions into the $4p^55p$ levels were measured from the ground level. Trajmar *et al.* [3] measured inelastic differential cross sections (DCSs) for excitation into a number of higher levels from the ground level. They obtained the integral cross sections by integrating the DCS over the scattering angle. Bogdanova and Yurgenson [4] used a pulsed electron beam to measure the excitation cross sections of $4p^55p$ levels from the ground level, attempting to eliminate the cascade contribution. Mityureva *et al.* [5] and Kolokolov *et al.* [6] measured the electron-impact excitation cross sections of Kr from the metastable level ($J=2$) to $4p^55p$ levels. Guo *et al.* [7] measured the DCS ratios for low-energy electron-impact excitation of the $4p^55s$ levels. Theoretical calculations have also been given to show the relativistic effects. Soon thereafter, Guo *et al.* [8,9] measured the DCSs for the excitation of $4p^55s$, $4p^55p$, $4p^54d$, and $4p^56s$ configurations. They used high-resolution electron energy-loss spectroscopy to obtain spectral intensities for the excitation. Theoretical investigations have also been carried out using the *R*-matrix method and unitarized first-order many-body theory. Chilton *et al.* [10] have measured the electron-impact excitation cross sections from the ground level of Kr by means of the optical method over a range of incident energies between onset and 250 eV. Recently, Jung *et al.* [11] measured the excitation cross sections out of the metastable levels of Kr into the levels of $4p^55p$ configuration. Their results showed that the peak excitation cross sections out of the two individual $4p^55s$ metastable levels are smaller than previous experimental data reported in the literature by one to two orders of magnitude.

Theoretically, most researches have been concentrated on elastic and inelastic cross sections to the lowest four levels of Kr $4p^55s$ configuration. Hyman [12] calculated the electron-impact excitation of metastable levels of atomic Kr using Born approximation [13] in the 1980s. Meneses *et al.* [14] calculated the differential and integrated cross sections for the electron-impact excitation of the levels of $4p^55s$ configuration at incident energies of 20, 30, 50, 60, and 100 eV. Kaur *et al.* [15] considered the excitation cross sections of Kr using a relativistic distorted-wave approximation. They obtained the differential and total cross sections for incident electrons in energy range from 15 to 100 eV. Yet they did not give results for separate levels. Fontes [16] calculated the electron-impact DCSs for metastable levels of Kr. Previous work before traditionally employed a single $4p^55s$ configuration to describe the lowest-lying excited levels. His work showed, however, that $4p^54d$ configuration plays a role in calculating the DCSs. Bartschat and Grum-Grzhimailo [17] investigated the electron-impact excitation of $4p^55s$ states at

15 eV using nonperturbative close-coupling-type models and a first-order perturbative distorted-wave approach. Their results showed that the results of close-coupling calculation agree better with the experiment than those of distorted wave method. Later, Dasgupta *et al.* [18,19] calculated the electron-impact excitation of Kr from the ground level and $4p^5 5s\ J=0$, 2 metastable states to the $4p^5 5s$ and $4p^5 5p$ manifolds using semirelativistic Breit-Pauli *R*-matrix method and first-order distorted-wave approximation.

For a long time, the agreement between theory and experiment has been poor. The experimental results published by different groups differ considerably as well. The recent accurate experimental results obtained by Jung *et al.* [11] give us an excellent opportunity to test the theory. When Jung *et al.* [11] compared their experiment with the most recent theoretical results [19], they pointed out that there is a potential problem with convergence of the theoretical calculations. All these show that theoretical calculations of the cross sections of Kr are challenging because of the complexity of the atomic structure of Kr and the complexity of the coupling of orbital and spin angular momenta of the outer electron with those of the core. This is particularly true for the excitation from the ground level because these cross sections are small. In the present paper, we study the electron-impact excitation cross section of atomic Kr using a close-coupling method implemented by a fully relativistic *R*-matrix method. Relativistic effects and channel coupling effects are naturally taken into account in this method. Special attention has been paid to the convergence of the cross sections, both from the expansion of the target atomic wave function and the number of partial wave summation. The results are compared with experimental and other theoretical results.

II. THEORETICAL METHODS

The *R*-matrix method for electron-atom and photon-atom interactions has been discussed in great detail by Burke *et al.*[20]. The present calculations have been carried out by using the fully relativistic *R*-matrix code DARC [21,22]. In an *R*-matrix calculation, the wave function of the $N+1$ electron system is given the form

$$\Psi_k(X_1 \cdots X_{N+1}) = \hat{A} \sum_{ij} c_{ijk} \Phi_i(X_1 \cdots X_N \hat{\mathbf{r}}_{N+1} \sigma_{N+1}) \times u_{ij}(r_{N+1}) + \sum_j d_{jk} \phi_j(X_1 \cdots X_{N+1}), \quad (1)$$

where $\hat{A}$ is the antisymmetrization operator to take the exchange effect between the target electrons and the free electron into account. X_i stands for the spatial ($\mathbf{r}_i$) and the spin (σ_i) coordinates of the ith electron. The functions $u_{ij}(r)$ under the first sum construct the basis sets for the continuum wave functions of the free electron, and Φ_i is the coupling between the target wave function of a specific level $J_i \pi_i$ and the angular and spin part of the free electron. The correlation functions ϕ_j in the second sum are constructed by the square integrable orbitals to account for the correlation effects not adequately considered because of the cutoff in the first sum.

In the relativistic *R*-matrix calculations, the square integrable orbitals are obtained from multiconfiguration Dirac-Fock (MCDF) code GRASP [23]. In the MCDF method, an atomic state is approximated by a linear combination of configuration state functions (CSFs) of the same symmetry

$$\Phi_\alpha(J\pi) = \sum_i^{n_c} a_i(\alpha) |\gamma_i J\pi\rangle, \quad (2)$$

where n_c is the number of CSFs and $a_i(\alpha)$ denotes the representation of the atomic state in this basis. The CSFs are antisymmetrized products of a common set of orthonormal orbitals which are optimized on the basis of the Dirac-Coulomb Hamiltonian. Further relativistic contributions to the atomic states due to Breit interactions are added by diagonalizing the Dirac-Coulomb-Breit Hamiltonian matrix. The dominant quantum electrodynamic contributions have also been included as a perturbation.

In the present work, the orbital wave functions are obtained by using an extended average level (EAL) method. The target wave functions of atomic Kr are described by following one-electron relativistic orbitals: $1s_{1/2}$, $2p_{1/2}$, $2p_{3/2}$, $3s_{1/2}$, $3p_{1/2}$, $3p_{3/2}$, $3d_{3/2}$, $3d_{5/2}$, $4s_{1/2}$, $4p_{1/2}$, $4p_{3/2}$, $5s_{1/2}$, $5p_{1/2}$, $5p_{3/2}$, $4d_{3/2}$, and $4d_{5/2}$. The wave functions of the first ten orbitals are obtained by optimizing the ground level $([\mathrm{Ni}]4s^2 4p^6)_0$. Other orbitals have been obtained by several separate optimizations corresponding to the levels with different total angular momentum and parity. As mentioned above, $4p^5 4d$ configuration plays a role in calculating the electron-impact excitation cross sections, thus we included $4d_{3/2}$ and $4d_{5/2}$ orbitals in the calculation. In this work, in addition to the configurations of $4s^2 4p^6$, $4s^2 4p^5 5s$, $4s^2 4p^5 5p$, and $4s^2 4p^5 4d$, we have included further configuration interaction (CI) among the following configurations: $4s^2 4p^4 5s^2$, $4s^2 4p^4 5s5p$, $4s^2 4p^4 4d5s$, $4s^2 4p^4 4d5p$, $4s^2 4p^4 5p^2$, $4s^2 4p^4 4d^2$, $4s4p^6 5s$, $4s4p^6 5p$, $4s4p^6 4d$, $4s4p^5 5s^2$, $4s4p^5 5s5p$, $4s4p^5 4d5s$, $4s4p^5 5p^2$, and $4s4p^5 4d^2$. In this way, the convergence of the wave-function expansion of target states should have been ensured. In performing the relativistic *R*-matrix calculation, the lowest 23 levels of atomic Kr are included in the expansion of wave function. Table I lists the lowest 23 levels and theoretical energies relative to the ground level. For comparison, the experimental values [24] have been given as well. It can easily be seen that the theory is in good agreement with the experiment.

In relativistic *R*-matrix calculations, the boundary was chosen to be 80 a.u. to ensure that the wave function is completely wrapped within the *R*-matrix sphere. Its size depends on a few factors: the atomic or ionic type, the numbers of the excited states and bound orbitals included in the calculation. In this work, the choice of 80 a.u. is large enough to ensure that the wave functions of all included orbitals are negligibly small at the boundary. This is also a measure to ensure the convergence of final results. For each angular momentum, the continuum orbitals are expressed as a linear combination of 28 numerical basis functions. To ensure the convergence of cross sections, we have calculated explicitly the maximal partial wave up to $J=39.5$. The contribution of higher partial waves has been included using a method described by Burgess [25,26].

TABLE I. Theoretical and experimental [24] energy levels (in Ry) for the target Kr relative to the ground level. For convenience, the Paschen notations have also been given for levels of $4p^5 5s$ and $4p^5 5p$ configurations.

No.	Paschen	Configuration	$J\pi$	Expt. [24]	Theory
1		$4s^2 4p^6$	0^e	0.0000	0.0000
2	$1s_5$	$4s^2 4p_{3/2}^{-1} 5s_{1/2}$	2°	0.7288	0.7266
3	$1s_4$	$4s^2 4p_{3/2}^{-1} 5s_{1/2}$	1°	0.7374	0.7376
4	$1s_3$	$4s^2 4p_{1/2}^{-1} 5s_{1/2}$	0°	0.7763	0.7788
5	$1s_2$	$4s^2 4p_{1/2}^{-1} 5s_{1/2}$	1°	0.7823	0.7890
6	$2p_{10}$	$4s^2 4p_{3/2}^{-1} 5p_{1/2}$	1^e	0.8307	0.8192
7	$2p_9$	$4s^2 4p_{3/2}^{-1} 5p_{1/2}$	0^e	0.8574	0.8395
8	$2p_8$	$4s^2 4p_{3/2}^{-1} 5p_{3/2}$	3^e	0.8410	0.8312
9	$2p_7$	$4s^2 4p_{3/2}^{-1} 5p_{3/2}$	2^e	0.8412	0.8378
10	$2p_6$	$4s^2 4p_{3/2}^{-1} 5p_{3/2}$	1^e	0.8472	0.8406
11	$2p_5$	$4s^2 4p_{3/2}^{-1} 5p_{3/2}$	2^e	0.8486	0.8416
12		$4s^2 4p_{3/2}^{-1} 4d_{3/2}$	0°	0.8818	0.8778
13		$4s^2 4p_{3/2}^{-1} 4d_{3/2}$	1°	0.8847	0.8809
14	$2p_4$	$4s^2 4p_{1/2}^{-1} 5p_{3/2}$	1^e	0.8894	0.8838
15		$4s^2 4p_{3/2}^{-1} 4d_{3/2}$	2°	0.8902	0.8847
16		$4s^2 4p_{3/2}^{-1} 4d_{5/2}$	4°	0.8912	0.8852
17	$2p_3$	$4s^2 4p_{1/2}^{-1} 5p_{1/2}$	1^e	0.8923	0.8867
18	$2p_2$	$4s^2 4p_{1/2}^{-1} 5p_{3/2}$	2^e	0.8925	0.8867
19		$4s^2 4p_{3/2}^{-1} 4d_{5/2}$	3°	0.8951	0.8898
20		$4s^2 4p_{3/2}^{-1} 4d_{3/2}$	1°	0.9080	0.8970
21	$2p_1$	$4s^2 4p_{1/2}^{-1} 5p_{1/2}$	0^e	0.9008	0.9004
22		$4s^2 4p_{3/2}^{-1} 4d_{5/2}$	2°	0.9009	0.9000
23		$4s^2 4p_{3/2}^{-1} 4d_{5/2}$	3°	0.9029	0.9031

III. RESULTS AND DISCUSSIONS

First, we check the convergence of cross sections on the number of partial waves. Generally speaking, the speed of convergence is different for different transitions. As an example, Fig. 1 shows the trend of convergence for excitation cross sections of transition $1s_5 \rightarrow 2p_6$ with the number of partial waves. The lines of 9.5, 19.5, 29.5, and 39.5 refer to cross sections by summing the contributions to cross sections of partial waves up to $J=9.5$, 19.5, 29.5, and 39.5, respectively. The solid line refers to the final results which includes further contributions of higher partial waves. The circle refers to the experimental results of Jung *et al.* [11]. It should be noted that Jung *et al.* measured the apparent cross sections which include both direct electron excitation into the level of interest and an additional cascade contribution from excitation into higher levels that decay into the level of interest. They estimated the cascade corrections will reduce the apparent cross sections by less than 10% for most transitions. It can be seen that the experimental cross sections are generally larger than our theoretical results. If we reduce the experimental results by 10%, which are represented by squares, then the theory is in good agreement with the experiment. From the inspection of Fig. 1, one can see that the cross sections converge very fast near the threshold. Below 2.5 eV,

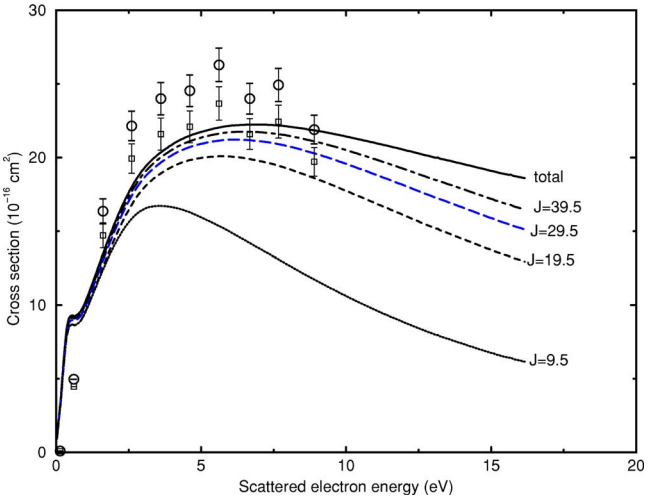

FIG. 1. (Color online) The convergence trend of excitation cross sections of transition $1s_5 \rightarrow 2p_6$ with the number of partial waves. The experimental data of Jung *et al.* [11] are denoted by circles with error bars being given, while the squares represent the experimental data reduced by 10% to correct the cascade contribution of higher levels.

the summation up to $J=9.5$ can get converged results. However, with the increasing of the scattered electron energy, the convergence becomes much slower. The higher the scattered electron energy is, the slower the cross section converges. At an energy of 15 eV, the cross sections obtained by summing the partial waves up to $J=39.5$ differ by about 10% from the final results which include contributions of further higher partial waves. From these discussions, we can conclude that our results have basically converged.

After having checked the convergence of the cross sections, we turn to the discussion of the elastic scattering cross sections and excitation cross sections. Figure 2 shows the elastic scattering cross sections for the ground level, (a), and the two metastable levels $1s_5$ and $1s_3$, (b) and (c), respectively. Obviously, the variational trend of the cross sections with scattered electron energy are different for the ground level and two metastable levels. For the ground level, elastic cross sections increase with scattered electron energy from zero. Near 20 eV, the cross sections show some structures and then continue to increase. For the two metastable levels, the cross sections near their thresholds are very large and then decrease rapidly with scattered electron energy.

Figures 3 and 4 show the excitation cross sections from the ground level to the levels of configurations $4p^5 5s$ and $4p^5 5p$, respectively. The dotted and dashed lines refer to the results of 51- and 15-state Breit-Pauli *R*-matrix (BP15) calculations obtained by Dasgupta *et al.* [18], respectively. When comparing our results with the corresponding results obtained by Dasgupta *et al.* [18], one can find that fair agreement is obtained between the theories. However, as their results of the *R*-matrix method and distorted wave approach differ considerably, we cannot give a definite conclusion. In Fig. 3, near the threshold, our calculated cross sections agree well with the theoretical results of Dasgupta *et al.* [18] obtained by the semirelativistic Breit-Pauli *R*-matrix method. However, with the increasing of the scattered electron en-

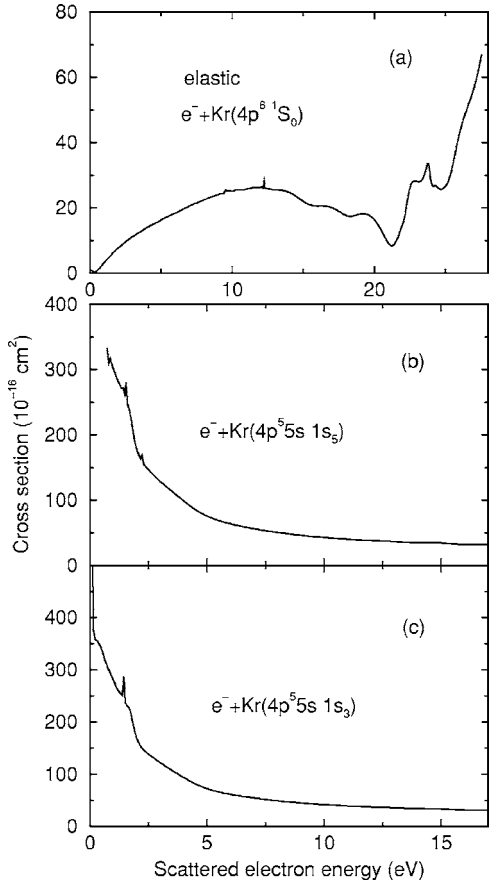

FIG. 2. The elastic scattering cross sections for the ground (a) and two metastable levels $1s_5$ and $1s_3$, (b) and (c), respectively, as a function of scattered electron energy.

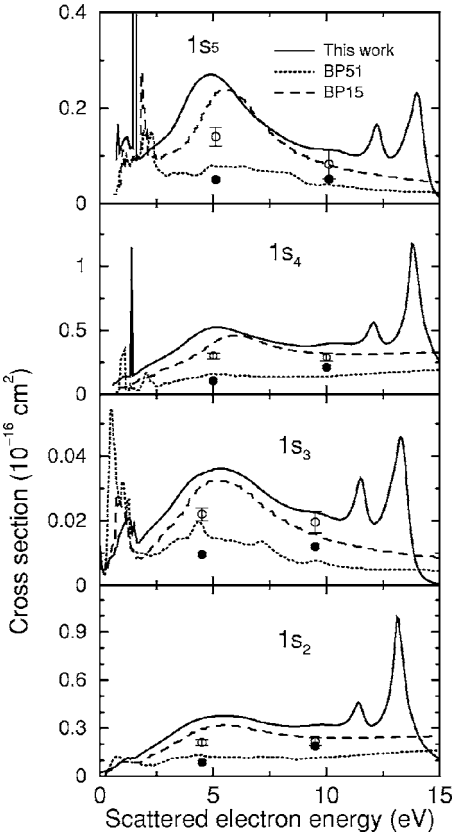

FIG. 3. The excitation cross sections from the ground level to the levels of $4p^5 5s$ configuration as a function of scattered electron energy (solid lines, this work). The dotted lines represent 51-state BP *R*-matrix calculation obtained by Dasgupta *et al.* [18]; dashed lines, 15-state BPRM results [18]. The experimental data are from Trajmar *et al.* [3] (solid circles) and Guo *et al.* [8] (open circles).

ergy, our calculated cross sections are larger than their results. In addition, our results show resonance structures in the energy range of 10–15 eV, which did not appear in the results obtained by Dasgupta *et al.* [18]. This is natural because we have included more CIs in the calculation. Comparing with the experiment, one can see that our cross sections are larger than but very close to the experimental data of Guo *et al.* [8] at the incident electron energy of 20 eV. For the two metastable levels, our predicted cross sections are just within the error bar. The cross sections of the BP51-state *R*-matrix calculation obtained by Dasgupta *et al.* [18] are lower than the experimental data and outside the error bar at this measured electron energy. At the incident electron energy of 15 eV, the differences are larger. The experimental data measured by Trajmar *et al.* [3] are smaller than our theoretical cross sections. Note that the two experimental data sets have substantial discrepancies, therefore it is not easy to evaluate the quality of different theoretical results.

Recently, Jung *et al.* [11] measured the excitation cross sections out of the metastable levels of Kr into the levels of the $4p^5 5p$ configuration. Before they published their work, experimental data obtained by different groups differed considerably and are much larger than the theoretical results [19]. Therefore the reliable experimental data by Jung *et al.* [11] should give us a good chance to test the theory. Figures 5–8 show the excitation cross sections from the levels of configuration $4p^5 5s$ to the levels of configuration $4p^5 5p$. Figures 5 and 7 refer to the results from the two metastable levels $1s_5$ and $1s_3$, respectively, while Figs. 6 and 8 refer to the results from other two levels $1s_4$ and $1s_2$, respectively. We first discuss the excitation cross sections from the two metastable levels. In Figs. 5 and 7, the dotted and dashed lines refer to 51- and 15-state BP *R*-matrix calculations obtained by Dasgupta *et al.* [19]. The experimental data obtained by Jung *et al.* [11] are denoted by circles. Note that to have a maximal coincidence with each other, the electron energy of the experimental data has been shifted the same value. It can easily be seen that the overall agreement between our theory and the experiment is good, both for the overall structures and for the absolute magnitude. In general, the theoretical cross sections are a little smaller than the experimental data. However, as mentioned above, Jung *et al.* [11] measured the apparent cross sections which include both direct electron excitation and an additional cascade contribution. The cascade corrections will reduce the apparent cross sections. If we take this factor into account, then our theoretical cross sections will be in better agreement with the experiment. For the six transitions which Jung *et al.* [11] have given their measured cross sections, the relative difference between the theoretical and experimental cross sections is about 10% for four transitions ($1s_5$-$2p_9$, $1s_5$-$2p_6$, $1s_3$-$2p_3$,

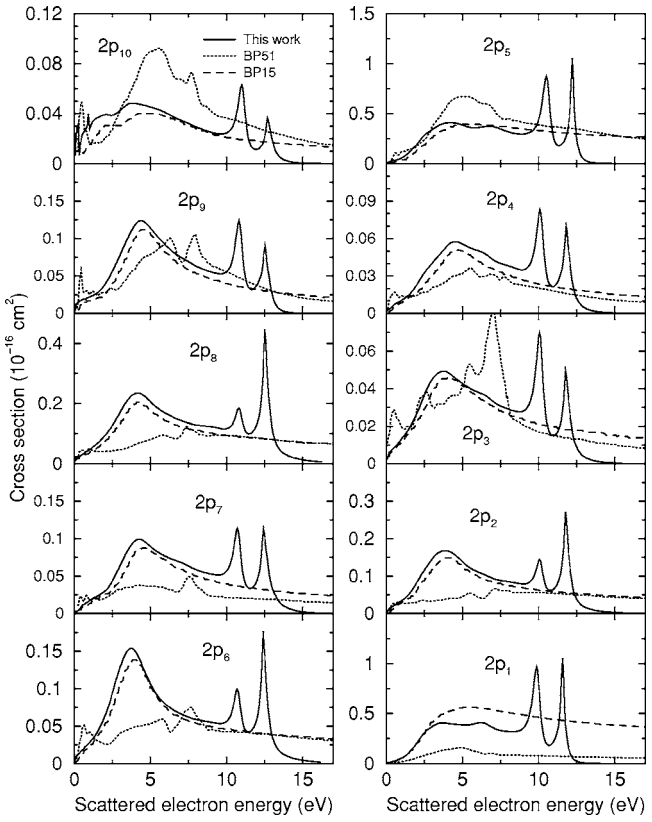

FIG. 4. The excitation cross sections from the ground level to the levels of $4p^5 5p$ configuration as a function of scattered electron energy (solid lines, this work). The dotted lines represent 51-state BP R-matrix calculation obtained by Dasgupta *et al.* [18]; dashed lines, 15-state BPRM results [18].

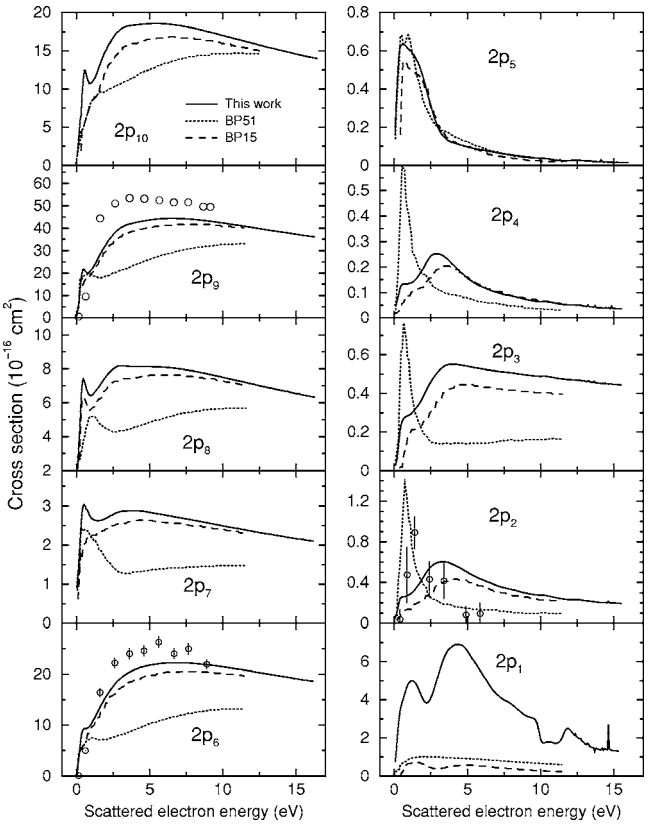

FIG. 5. The excitation cross sections from the metastable level $1s_5$ to the levels of $4p^5 5p$ configuration as a function of scattered electron energy (solid lines, this work). The dotted lines represent 51-state BP R-matrix calculation obtained by Dasgupta *et al.* [19]; dashed lines, 15-state BPRM results [19]. The circles are experimental results obtained by Jung *et al.* [11].

and $1s_3$-$2p_1$). For the transition of $1s_3$-$2p_2$, both theory and experiment show similar variational trend, in which cross sections decrease fast with electron energy. The theory predicts the peak cross section to be 1.1×10^{-15} cm^2, while the measured peak cross section is 1.75×10^{-15} cm^2. The theoretical value is nearly 40% lower than experimental value, which is outside the error bar. For the transition of $1s_5$-$2p_2$, however, the overall structure predicted by theory is different from the measured. The theory shows a broad structure and the cross sections decrease slow with electron energy, while the experiment measured a narrow structure and the cross sections decrease fast with energy. The results of BP15 obtained by Dasgupta *et al.* [19] predicted the same varational trend of cross section with our results.

Besides the cross sections for the six transitions, Jung *et al.* [11] also measured cross sections at 3.5 eV for other transitions out of the metastable levels. As they discussed in their work, the shapes of the excitation cross sections out of the metastable levels of Kr as a function of electron energy fall into two main categories. For core-preserving, dipole-allowed excitations, there is broad energy dependence with a peak around 6 eV. The other shape is for the core-preserving, dipole-forbidden excitations which have a sharp peak at 3 eV. Therefore the cross sections at 3.5 eV should be very close to the peak values. In Table II we list our theoretical peak cross sections for transitions $1s_y$-$2p_x$ from the metastable levels compared to the experimental data [11]. It can easily be seen that our predicted peak cross sections are in agreement with the measured values at 3.5 eV. For most transitions, the theoretical values are smaller than experiment. Yet they are bigger than experiment for transitions of $1s_5\rightarrow2p_3$, $1s_5\rightarrow2p_5$, $1s_5\rightarrow2p_6$, and $1s_5\rightarrow2p_{10}$. The theoretical values are within the error bars except for transition of $1s_5\rightarrow2p_5$ (0.63×10^{-16} cm^2), which is just outside the error bar [$(0.4\pm0.2)\times10^{-16}$ cm^2].

Comparing our theoretical results with other experimental results [5,6], we found that these experimental data are much larger than our theoretical cross sections. The excitation cross sections measured in these experiments are between 10 and 20 times larger than the experimental data obtained by Jung *et al.* [11]. Thus we did not give these experimental data [5,6] in the figures. Theoretical results, however, do not differ so much. Dasgupta *et al.* [19] calculated the cross sections out of the two metastable levels using two different distorted-wave (DW-1 and DW-2) and BP R-matrix close-coupling method with 15 basis functions (BP15) and with 51 basis functions (BP51). Though these four calculations predicted different cross sections, the results have basically the same order of magnitude. Their results of BP51 should in principle be more accurate than those of BP15, yet the cross sections predicted by BP51 are much smaller than the experi-

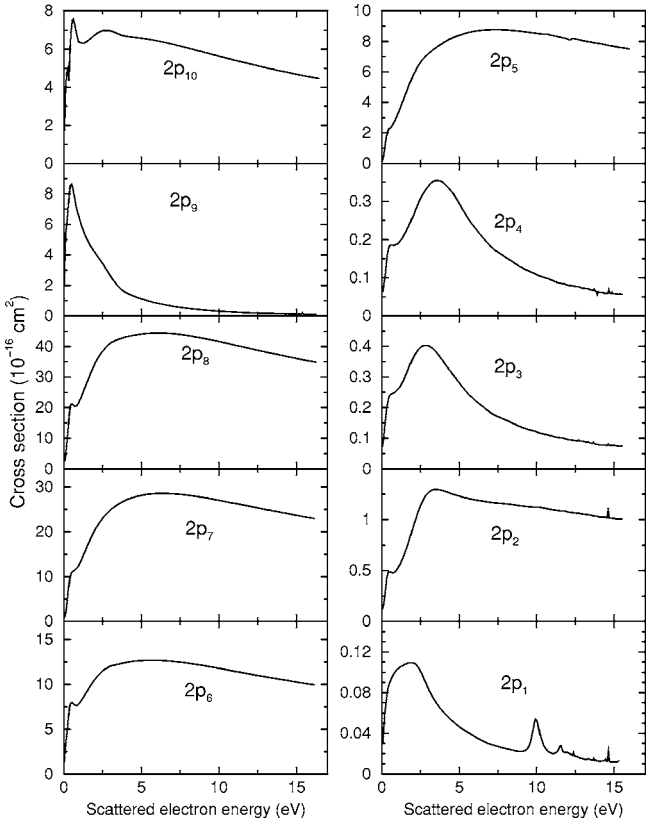

FIG. 6. The excitation cross sections from the metastable level $1s_4$ to the levels of $4p^5 5p$ configuration as a function of scattered electron energy.

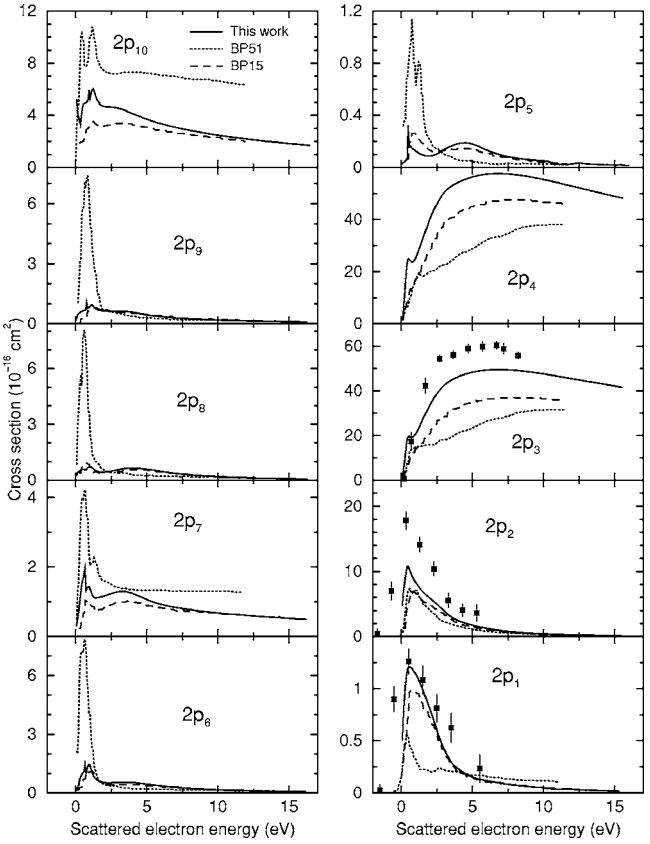

FIG. 7. The excitation cross sections from the metastable level $1s_3$ to the levels of $4p^5 5p$ configuration as a function of scattered electron energy (solid lines, this work). The dotted lines represent 51-state BP *R*-matrix calculation obtained by Dasgupta *et al.* [19]; dashed lines, 15-state BPRM results [19]. The circles are experimental results obtained by Jung *et al.* [11].

mental data of Jung *et al.* [11]. It is suggested that the results of BP51 have not converged. On the contrary, *R*-matrix calculation of BP15 agrees better than the results of BP51 with experimental data [11]. Even so, the predicted cross sections out of the $1s_3$ level predicted by BP15 are generally smaller than experimental data by about 40%. For the transition of $1s_3 \rightarrow 2p_2$, this value reaches 55%.

TABLE II. Comparison of the theoretical peak cross sections with those measured cross sections (in 10^{-16} cm^2) at 3.5 eV for transitions of $1s_y \rightarrow 2p_x$. Error bars include both statistical uncertainties and the ±35% uncertainties in the absolute calibration of the $2p_9$ level in the experiment.

Excitation	Peak cross section	Q (3.5 eV)
$1s_3 \rightarrow 2p_1$	1.2	1.3±0.5
$1s_3 \rightarrow 2p_2$	11.0	16±6
$1s_5 \rightarrow 2p_2$	0.6	0.9±0.4
$1s_3 \rightarrow 2p_3$	50.0	55±21
$1s_5 \rightarrow 2p_3$	0.55	0.5±0.3
$1s_3 \rightarrow 2p_4$	58.0	64±25
$1s_5 \rightarrow 2p_5$	0.63	0.4±0.2
$1s_5 \rightarrow 2p_6$	22.3	21±7
$1s_5 \rightarrow 2p_7$	2.9	3.2±1.1
$1s_5 \rightarrow 2p_8$	8.2	8.9±3.1
$1s_5 \rightarrow 2p_9$	45.0	52±18
$1s_5 \rightarrow 2p_{10}$	18.6	15±7

Why do the results of BP15 agree better with the experiment than those of BP51? Frankly speaking, we do not know the exact reasons because we do not know the details in the calculations carried out by Dasgupta *et al.* [18,19] such as the number of partial waves included in their work. One possibility may be that they have included inadequate summation of partial waves in their calculations. As we know, for some atoms or atomic ions, inclusion of more CI could reduce the excitation cross sections [27–29]. For example, Griffin *et al.* [27] studied the electron impact excitation of Fe VIII using the BP *R*-matrix method. Their results show that inclusion of more CI can result in substantial reduction of excitation cross section. If Dasgupta *et al.* [18,19] have included the same number of partial waves in their BP51 and BP15 calculations, then it is easy to understand why their results of BP51 are smaller than those of BP15 in most energy regions. If they include more contribution of partial waves, then the results of BP51 should increase. Then the results of BP51 will agree better with the experiment. Therefore, to obtain accurate excitation cross section, it is important to take into account of all factors such as adequate CI, enough number of partial waves, and relativistic effects.

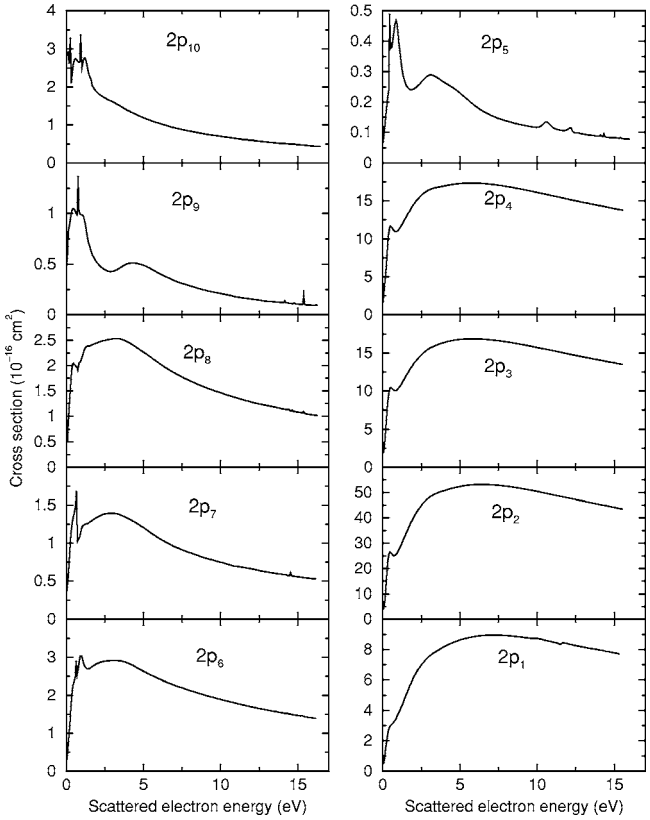

FIG. 8. The excitation cross sections from the metastable level $1s_2$ to the levels of $4p^5 5p$ configuration as a function of scattered electron energy.

Comparing Figs. 5 and 7 with Fig. 4, one can see that the cross sections out of the metastable levels are much larger than the corresponding results from the ground level. This is in agreement with the experimental results [11] that the peak cross sections are 10–1600 times larger than the corresponding cross sections out of the ground level. For example, the peak cross section for transition of $1s_3 \rightarrow 2p_4$ is 5.8×10^{-15} cm^2, which is about 1000 times larger than the result from the ground level.

The other two levels $1s_4$ and $1s_2$ of $4p^5 5s$ configuration are dipole-allowed to the ground level. The cross sections of these two levels are given in Figs. 6 and 8, respectively. As far as we know, there are no experimental data for these transitions. Few theoretical studies have been carried out, either. It is believed that the excitation cross sections of these transitions can be measured in the future. Some transitions have large cross sections, such as $1s_4 \rightarrow 2p_8$, $1s_4 \rightarrow 2p_7$, and $1s_4 \rightarrow 2p_6$. They have peak cross sections of 4.5×10^{-15}, 2.9×10^{-15}, and 1.3×10^{-15} cm^2, respectively. For the transitions of $1s_2 \rightarrow 2p_4$, $1s_2 \rightarrow 2p_3$, and $1s_2 \rightarrow 2p_2$, the peak values are 1.75×10^{-15}, 1.7×10^{-15}, and 5.4×10^{-15} cm^2, respectively. The large cross sections for these transitions should be able to be measured if one can control the short lifetime levels in the experiment.

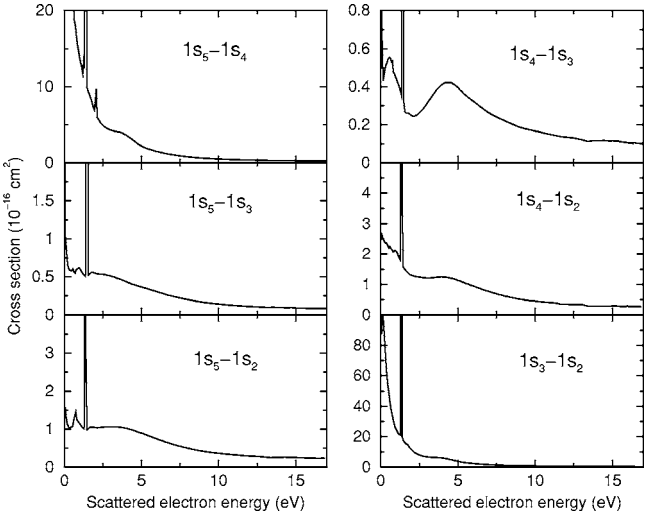

FIG. 9. The excitation cross sections for transitions between the levels of $4p^5 5s$ configuration: $1s_5$-$1s_4$, $1s_5$-$1s_3$, $1s_5$-$1s_2$, $1s_4$-$1s_3$, $1s_4$-$1s_2$, and $1s_3$-$1s_2$.

Figure 9 shows excitation cross sections for transitions among the levels of $4p^5 5s$ configuration: $1s_5$-$1s_4$, $1s_5$-$1s_3$, $1s_5$-$1s_2$, $1s_4$-$1s_3$, $1s_4$-$1s_2$, and $1s_3$-$1s_2$. There is a reasonable agreement with the theoretical results obtained by Dasgupta *et al.* [19] using the *R*-matrix calculation. However, we predict a strong resonance near the threshold. This may be due to the bigger wave-function expansion in our target states. We have included many double and high excited states in the description of the target, yet Dasgupta *et al.* [19] have not.

To summarize, we have investigated the electron-impact excitation cross sections at low electron energies using a fully relativistic *R*-matrix method. Special attention has been paid to ensure the convergence of final results. The predicted overall structures agree well with a recent experiment except for the transition of $1s_5$-$2p_2$. Further, the magnitude of theoretical cross sections are in good agreement with the experimental data after shifting the position of the electron energy. Present results eliminated the significant discrepancies between theory and past experimental work before Jung *et al.* The experimental cross sections published before Jung *et al.* are at least an order of magnitude larger than both our theoretical results and the experimental data of Jung *et al.* for transitions out of the metastable levels. Different theoretical work, however, predicted the same order of magnitude for the excitation cross sections.

ACKNOWLEDGMENTS

This work was supported by the National Science Fund for Distinguished Young Scholars under Grant No. 10025416, the National Natural Science Foundation of China under Grant Nos. 10204024, 10373014, 10433010, and 10474138.

[1] V. Milosavljevic, S. Djenize, and M. S. Dimitrijevic, Phys. Rev. E **68**, 016402 (2003).
[2] P. V. Feltsan, Ukr. Fiz. Zh. (Russ. Ed.) **12**, 1425 (1967).
[3] S. Trajmar, S. K. Srivastava, H. Tanaka, H. Nishimura, and D. C. Cartwright, Phys. Rev. A **23**, 2167 (1981).
[4] I. P. Bogdanova and S. V. Yurgenson, Opt. Spectrosc. **62**, 424 (1987).
[5] A. A. Mityureva, N. P. Penkin, and V. V. Smirnov, Opt. Spectrosc. **67**, 461 (1989).
[6] N. B. Kolokolov and O. V. Terekhova, Opt. Spectrosc. **86**, 481 (1999).
[7] X. Z. Guo, M. A. Khakoo, D. F. Mathews, G. Mikaeliant, A. Crowe, K. Kanik, S. Trajmar, V. Zeman, K. Bartschat, and C. J. Fontes, J. Phys. B **32**, L155 (1999).
[8] X. Z. Guo, D. F. Mathews, G. Mikaelian, M. A. Khakoo, A. Crowe, I. Kanik, S. Trajmar, V. Zeman, K. Bartschat, and C. J. Fontes, J. Phys. B **33**, 1895 (2000).
[9] X. Z. Guo, D. F. Mathews, G. Mikaelian, M. A. Khakoo, A. Crowe, I. Kanik, S. Trajmar, V. Zeman, K. Bartschat, and C. J. Fontes, J. Phys. B **33**, 1921 (2000).
[10] J. E. Chilton, M. D. Stewart, and C. C. Lin, Phys. Rev. A **62**, 032714 (2000).
[11] R. O. Jung, T. E. Stone, J. B. Boffard, L. W. Anderson, and C. C. Lin, Phys. Rev. Lett. **94**, 163202 (2005).
[12] H. A. Hyman, Phys. Rev. A **18**, 441 (1978).
[13] B. L. Moiseiwitsch and S. J. Smith, Rev. Mod. Phys. **40**, 238 (1968).
[14] G. D. Meneses, F. J. da Paixao, and N. T. Padial, Phys. Rev. A **32**, 156 (1985).
[15] S. Kaur, R. Srivastava, R. P. McEachran, and A. D. Stauffer, J. Phys. B **31**, 4833 (1998).
[16] C. Fontes, J. Phys. B **31**, 175 (1998).
[17] K. Bartschat and A. N. Grum-Grzhimailo, J. Phys. B **33**, 4603 (2000).
[18] A. Dasgupta, K. Bartschat, D. Vaid, A. N. Grum-Grzhimailo, D. H. Madison, M. Blaha, and J. L. Giuliani, Phys. Rev. A **64**, 052710 (2001).
[19] A. Dasgupta, K. Bartschat, D. Vaid, A. N. Grum-Grzhimailo, D. H. Madison, M. Blaha, and J. L. Giuliani, Phys. Rev. A **65**, 042724 (2002).
[20] P. G. Burke, A. Hibbert, and W. D. Robb, J. Phys. B **4**, 153 (1971).
[21] P. H. Norrington and I. P. Grant, J. Phys. B **20**, 4869 (1987).
[22] W. P. Wijesundera, F. A. Parpia, I. P. Grant, and P. H. Norrington, J. Phys. B **24**, 1803 (1991).
[23] K. G. Dyall, I. P. Grant, C. T. Johnson, F. A. Parpia, and E. P. Plummer, Comput. Phys. Commun. **55**, 425 (1989).
[24] See NIST Atomic Spectra Data Base, http://physics.nist.gov/cgi-bin/AtData/main_asd
[25] A. Burgess, J. Phys. B **7**, L364 (1974).
[26] A. Burgess, D. G. Hummer, and J. A. Tully, Philos. Trans. R. Soc. London, Ser. A **266**, 255 (1970).
[27] D. C. Griffin, M. S. Pindzola, and N. R. Badnell, Astron. Astrophys. **142**, 317 (2000).
[28] Jiaolong Zeng, G. Y. Liang, G. Zhao, and J. R. Shi, Mon. Not. R. Astron. Soc. **357**, 440 (2005).
[29] Jianmin Yuan, Phys. Rev. A **61**, 012704 (2000).